SMC-TR-95-52

AEROSPACE REPORT NO.
TR-95(5530)-2

New Solar Flare Particle Environment Models and Titan/Centaur INU Multiple-Bit Single Event Upset Rates

1 December 1995

Prepared by

T. J. LIE
Electrical and Electronic Systems Department
Electronics Systems Division
Engineering and Technology Group

and

W. A. KOLASINSKI
Space and Environment Technology Center
Technology Operations
Engineering and Technology Group

Prepared for

SPACE AND MISSILE SYSTEMS CENTER
AIR FORCE MATERIEL COMMAND
2430 E. El Segundo Boulevard
Los Angeles Air Force Base, CA 90245

Contract No. F04701-93-C-0094

Space Systems Group

THE AEROSPACE CORPORATION
El Segundo, California

This report was submitted by The Aerospace Corporation, El Segundo, CA 90245-4691, under Contract No. F04701-93-C-0094 with the Space and Missile Systems Center, Los Angeles Air Force Base, CA 90245. It was reviewed and approved for The Aerospace Corporation by J. M. Straus, Acting Principal Director, Electronics and Power Subdivision. Lt. Col. Adrian Gomez was the project officer.

This report has been reviewed by the Public Affairs Office (PAS) and is releasable to the National Technical Information Service (NTIS). At NTIS, it will be available to the general public, including foreign nationals.

This technical report has been reviewed and is approved for publication. Publication of this report does not constitute Air Force approval of the report's findings or conclusions. It is published only for the exchange and stimulation of ideas.

Lt. Col. Adrian Gomez
Chief, Titan Upper Stage IPT

REPORT DOCUMENTATION PAGE

Form Approved
OMB No. 0704-0188

1. AGENCY USE ONLY (*Leave blank*)	2. REPORT DATE	3. REPORT TYPE AND DATES COVERED
	1 December 1995	

4. TITLE AND SUBTITLE
New Solar Flare Particle Environment Models and Titan/Centaur INU Multiple-Bit Single Event Upset Rates

5. FUNDING NUMBERS
F04701-93-C-0094

6. AUTHOR(S)
Lie, T. J.; and Kolasinski, W. A.

7. PERFORMING ORGANIZATION NAME(S) AND ADDRESS(ES)
The Aerospace Corporation
Electronic Systems Division and Technology Operations
El Segundo, CA 90245-4691

8. PERFORMING ORGANIZATION REPORT NUMBER
TR-95(5530)-2

9. SPONSORING/MONITORING AGENCY NAME(S) AND ADDRESS(ES)
Space and Missile Systems Center
Air Force Materiel Command
2430 E. El Segundo Blvd.
Los Angeles Air Force Base, CA 90245

10. SPONSORING/MONITORING AGENCY REPORT NUMBER
SMC-TR-95-52

11. SUPPLEMENTARY NOTES

12a. DISTRIBUTION/AVAILABILITY STATEMENT
Approved for public release; distribution unlimited

12b. DISTRIBUTION CODE

13. ABSTRACT (*Maximum 200 words*)

Recently acquired solar flare data have been used to revise particle environment models for the August 1972 and October 1989 events. The revised models are presented, together with their composite event model and the average flare model. These models are applied to calculate the rates of single- and multiple-bit single event upsets (SbSEUs and MbSEUs) during solar flares for the Titan/Centaur inertial navigation unit (INU) in an orbit of 26.6° inclination for a 6-hour geosynchronous orbit (GSO) transfer mission. Since shielding has been found to enhance immunity to solar flare SEU, the effect of the inherently present anisotropic shielding distributions was studied, including shielding by printed circuit board components. The INU's SEU requirement of a 25,000 hour mean-time-between-failures (MTBF) is satisfied when the proton integral flux above 50 MeV falls below 30 pfu [1 pfu (particle flux unit) is 1 proton/cm2/sec/steradian], which corresponds to the peak integral flux of a three-times average flare. For the referred Titan/Centaur mission, we recommend that the current solar activity launch NO-GO criterion of 10 pfu be changed to 30 pfu. This change should reduce the average number of NO-GO days per year from 24 to 14.

14. SUBJECT TERMS
Single Event Upset
Solar Flare
Titan/Centaur

15. NUMBER OF PAGES
43

16. PRICE CODE

17. SECURITY CLASSIFICATION OF REPORT	18. SECURITY CLASSIFICATION OF THIS PAGE	19. SECURITY CLASSIFICATION OF ABSTRACT	20. LIMITATION OF ABSTRACT
Unclassified	Unclassified	Unclassified	

Preface

We would like to thank Dr. H. Sauer of the National Oceanic and Atmospheric Administration for kindly providing us the recent solar flare data. Dr. J. B. Blake, Director of Space Particles and Fields Department, initiated this work and encouraged us to carry on. The work was supported by the Titan Avionics Directorate.

Contents

Figures

Tables

1. Introduction

Multiple-bit single event upsets (MbSEUs) are generally of concern to space programs because standard Error Detection and Correction (EDAC) codes can correct only single-bit single event upsets (SbSEUs) per word. An MbSEU is caused either by the passage of a single particle through two or more memory bits in the same word, or by two or more particles, each randomly striking one of these bits within a vulnerable time span, i.e., duty cycle, of the circuit operation. Since the duty cycle is generally very short, the probability for the second type of error is much smaller than for the first. Thus, in what follows, the term MbSEU refers exclusively to MbSEUs caused by single particle strikes.

The possibility of MbSEUs was first pointed out by Blake and Mandel in their observation of SEU multiplicities within 1K static random access memory (SRAM) chips on a low altitude satellite in polar orbit.[1] While much less probable than ordinary SbSEUs, the MbSEUs might pose especially serious problems during a solar flare, where the energetic, heavy ion flux may occasionally exceed the ambient intensity by several orders of magnitude. For example, it has been shown that the Titan/Centaur MbSEU rate behind 100 mils of aluminum shielding is roughly 1000 times higher during a flare like the August 1972 (Aug72) event, than during the no-flare, 90% worst-case interplanetary weather condition.[2]

Solar flares occur during the 7-year active period of every 11-year solar cycle. Since flares pose a serious threat to spacecraft systems, it is of great practical interest to establish the probability of encountering a given magnitude flare during a space mission. Feynman, Spitale, and Wang have studied this problem in considerable detail.[3] Some pertinent results of their work are summarized in Appendix A. Using these results, we deduce that above-average-sized flares, i.e., those resulting in a total fluence of more than 7.3E+07 protons/cm^2 with energies above 10 MeV, occur approximately 3.4 times per active year. Similarly, flares like the Aug72 or the October 1989 (Oct89) events, yielding a fluence greater than 1E+10 protons/cm^2 with energies above 10 MeV, happen roughly 0.09 times per active year, or once in 11 active years.

Recently, solar-flare proton data for the current 22nd solar cycle have been published by the National Oceanic and Atmospheric Administration (NOAA).[4] Also, half-hourly fluence data were kindly provided to us by NOAA for the Oct89 solar flare, by far the largest one during the solar cycle.[4] We have augmented the published Aug72 flare data[5] with low energy data obtained from Lockheed.[6] For all cases published in the NOAA paper,[4] the energy spectra (fluence as a function of energy) above 100 MeV are considerably harder than had been supposed in the past. At energies below 10 MeV, both the NOAA and Lockheed data show a much more rapid increase of the flux with decreasing energy than that provided by the existing model, as implemented in the SPACE RADIATION (SPACERAD) code.[6]

The differences between the existing solar flare models and the recent solar flare data have prompted us to define a new set of proton fluence models for the Aug72 and Oct89 events as well as for a composite event. These models were used to revisit previous Titan/Centaur MbSEU rate calculations performed at Aerospace,[2] for which the mean solar flare proton fluence models were used.[7] Following up on the observation of Chenette and Dietrich that shielding can be quite effective in reducing solar flare SEU,[8] we have extended the previous

calculation, originally performed only for 100 mils of aluminum shielding, to a number of thicknesses ranging between 0 and 1000 mils.

For MbSEU shielding, the silicon materials of microelectronic packages on the printed circuit boards (PCBs) provide a significant contribution; silicon has practically the same shielding effectiveness as aluminum. In order to calculate this contribution, a new computer code, MbSEU_PCB, was developed to perform the SEU analyses for anisotropic shielding distributions on PCBs. The code was used to estimate the MbSEU survivability of the inertial navigation unit (INU) on a Titan/Centaur transfer orbit during the peak hours of an Aug72 event, and also of an average solar flare event as described in Appendix B.

The report is presented in the following order. In Section 2, the new and the old data are compared, and some new solar proton-fluence models based on least-squares fits to the data are proposed. In Section 3, the heavy ion environments generated on the basis of the new solar flare models are described. In Section 4, the results of MbSEU rate calculations for IDT's 256K SRAM (IDT71256) in the Aug72 and Oct89 flare environments are discussed. In Section 5, these results are used to assess the MbSEU vulnerability of the INU during an Aug72 event, as well as during an average-sized event, as defined in Appendix B. In Section 6, the summary and conclusions are presented. Finally, in Appendices A and B, respectively, the solar flare proton-fluence statistics are described, [3] and the average solar flare in terms of proton fluence is defined.

Note that in this report, all calculations related to the Titan/Centaur mission refer to the 6-hour geosynchronous orbit (GSO) transfer mission with the transfer orbit of 26.6° inclination.

2. Proton Fluence and Peak Flux During August 1972 and October 1989 Flares

Examples of the recent NOAA data are displayed in Figures 1 and 2.[4] Figure 1 shows the integral proton fluences as functions of energy for three consecutive solar flares in the August–October 1989 time period. Since the Oct89 event is by far the largest event in this solar cycle, we have singled it out for comparison with the Aug72 event in the subsequent presentation.

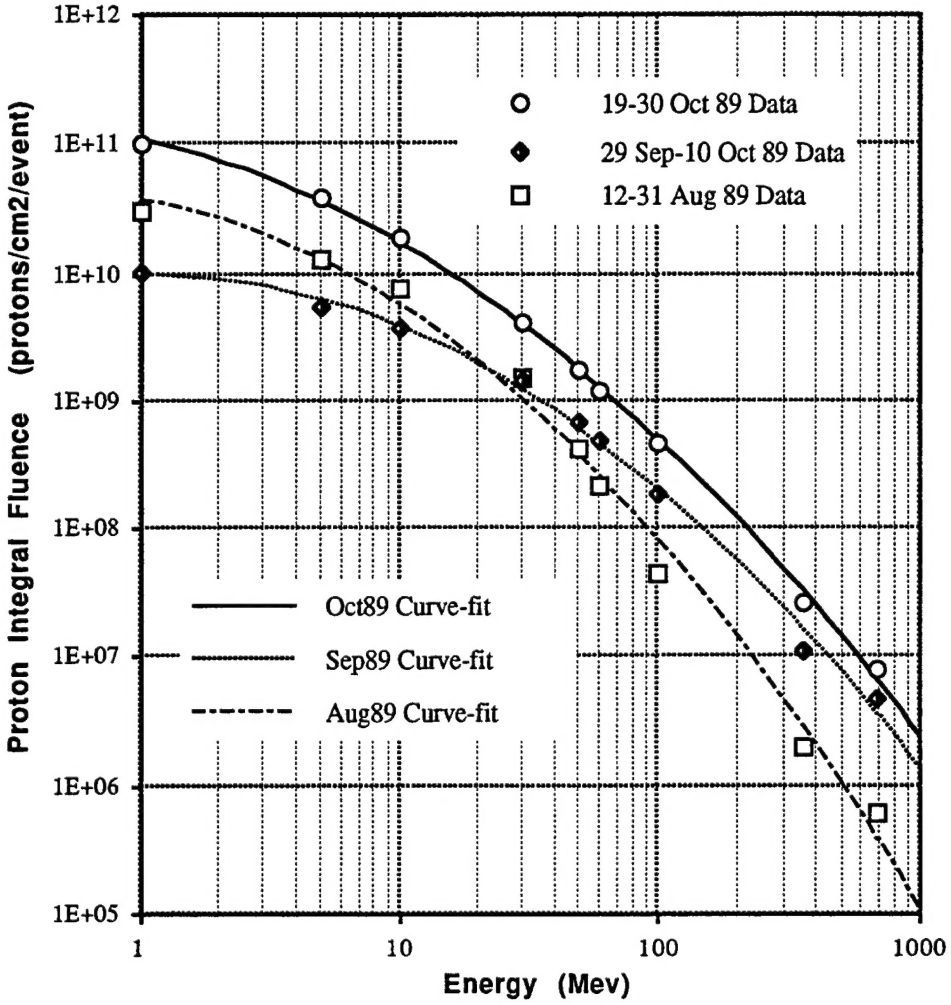

Figure 1. Integral Proton Fluence of Three Solar Flares of August–October 1989

Figure 2 shows the time history of the Oct89 event during the first 3 days, starting on October 19. Each data point represents the flux averaged over 30 minutes. A peak-flux period of approximately 6 hours is clearly visible. During that period, the flux is close to 10 times higher than at any other time within the event.

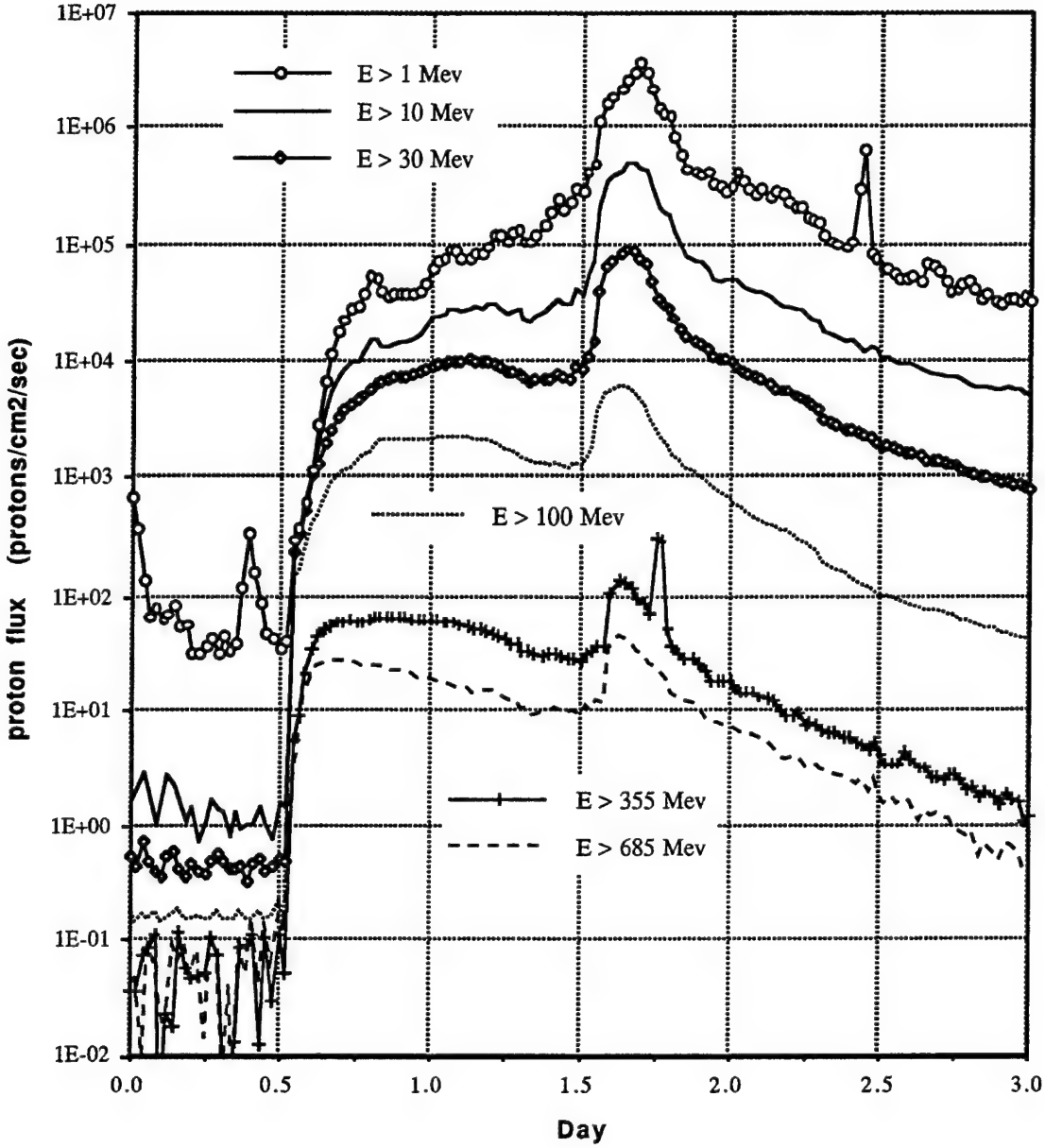

Figure 2. Temporal Proton Flux Development of Oct89 Solar Flare (first 3 days of October 19–30)

Figure 3 shows the total integral proton fluences associated with the Oct89 and Aug72 events, together with a composite event fluence, arrived at by combining the worst-case features of both data sets as functions of energy. The Aug72 data are a combination of data from References 5 and 9; there is excellent agreement between these two data sets in the energy range of overlap. Also included in Figure 3 is a plot of the SPACERAD formula for Aug72,[6] which is an extrapolation of the King formula,[9] based on a fit to data in the 10–100 MeV energy range.

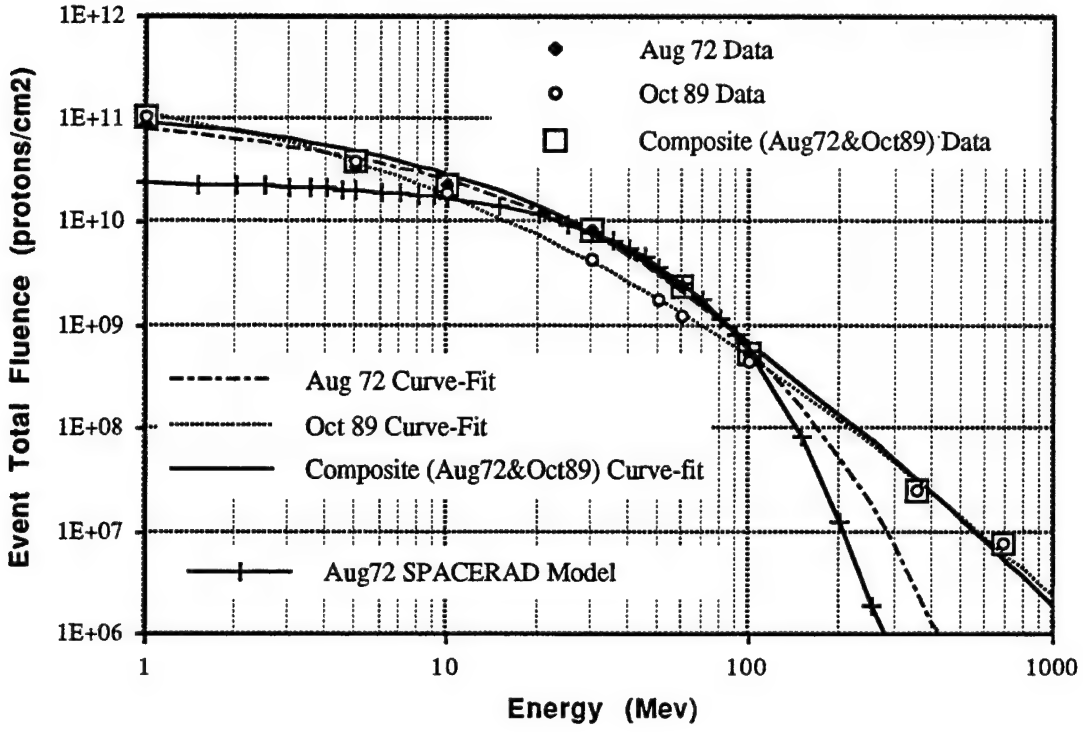

Figure 3. Event Total Proton Integral Fluence of Aug72 and Oct89 Solar Flare Events and Their Composite Event in Geosynchronous Orbits

The curves drawn through the respective sets of data points are plots of analytical expressions whose constants were determined by performing least-squares fits to the data. These expressions are as follows, where F is the fluence in protons/cm^2/event and R_p is the proton rigidity, $R_p=\sqrt{(E^2+2m_pE)}$, in megavolts (MV), with energy E and proton mass m_p in mega-electron-volts (MeV):

(a) Aug72 Event Total Fluence:

$$F = 1.32\times10^{11}\times exp\left(-R_p/82.76\right), \quad 1\le E\le 1000\,MeV \tag{1}$$

(b) Oct89 Event Total Fluence:

$$\begin{aligned} F &= 2.04\times10^{11}\times exp\left(-R_p/61.53\right), && 1\le E\le 30\,MeV \\ &= 5.02\times10^{18}\times R_p^{-3.8}, && 30 < E\le 1000\,MeV \end{aligned} \tag{2}$$

(c) Composite Event Total Fluence of Aug72 and Oct89 Events:

$$\begin{aligned} F &= 1.67\times10^{11}\times exp\left(-R_p/79\right), && 1\le E\le 60\,MeV \\ &= 2.94\times10^{20}\times R_p^{-4.4}, && 60 < E\le 1000\,MeV \end{aligned} \tag{3}$$

(d) Aug72 SPACERAD Total Fluence:

$$F = 2.45 \times 10^{10} \times exp(-E/26.5), \qquad 1 \le E \le 1000\,MeV \tag{4}$$

Note that the Aug72 fluence data are extremely well represented by a single expression that is an exponential in rigidity, whereas in the Oct89 case, a power-law dependence on rigidity is needed to fit the data above 30 MeV.

Comparison of the SPACERAD model with the Aug72 and Oct89 models shows that the former considerably underestimates the proton fluence both at low (<10 MeV) and high (>100 MeV) energy. At high energy, this underestimation results in reduced SEU assessments as shielding thickness increases. This is illustrated in Figure 4. In this figure, with a sample Fairchild device 93425A, the proton-induced SEUs during the solar flares are calculated in a 450 nmi altitude polar orbit. The proton SEUs per SPACERAD model decrease rapidly as the shielding thickness increases beyond 500 mils.

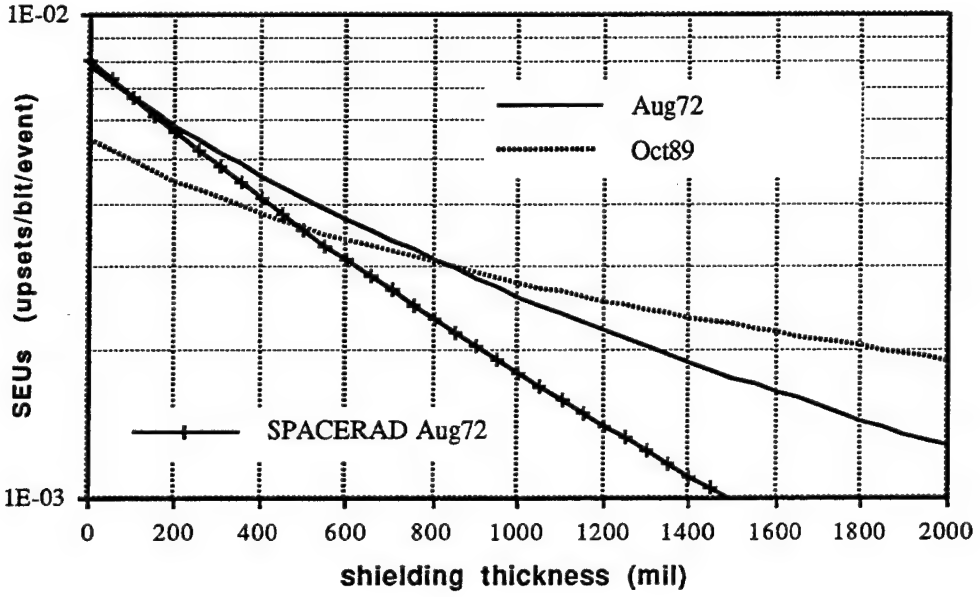

Figure 4. Proton-Induced SEUs of Fairchild's 93425A Device at 450 nmi Altitude Polar Orbit During Solar Flares

In the preceding discussion, models pertaining to total-event fluence were presented and summarized in Figure 3. However, as can be discerned from Figure 2, the peak flux, rather than total fluence, often has more bearing on system vulnerability. With this in mind, peak-flux data and models derived from the data are presented below.

Figure 5 shows the peak fluxes of the solar flare protons during the Aug72 and Oct89 events. As before, the smooth curves through the data points are plots of the following expressions, where J is the integral flux in protons/cm^2/second, E the energy in MeV, and R_p is the proton rigidity in MV:

(a) Aug72 Peak Flux:

$$J = 5.44\times10^{6}\times exp\left(-R_p/75.8\right), \qquad 1\le E\le 1000\,MeV \tag{5}$$

(b) Oct89 Peak Flux:

$$\begin{aligned} J &= 7.93\times10^{6}\times exp\left(-R_p/53\right), && 1\le E\le 30\,MeV \\ &= 4.71\times10^{15}\times R_p^{-4.51}, && 30< E\le 1000\,MeV \end{aligned} \tag{6}$$

(c) Aug72 SPACERAD Peak Flux:

$$\begin{aligned} J &= 1.17\times10^{6}\times exp\left(-R_p/100\right)-1.48\times10^{3}, && 1\le E\le 150\,MeV \\ &= 2.76\times10^{25}\times R_p^{-8}, && 150< E\le 1000\,MeV \end{aligned} \tag{7}$$

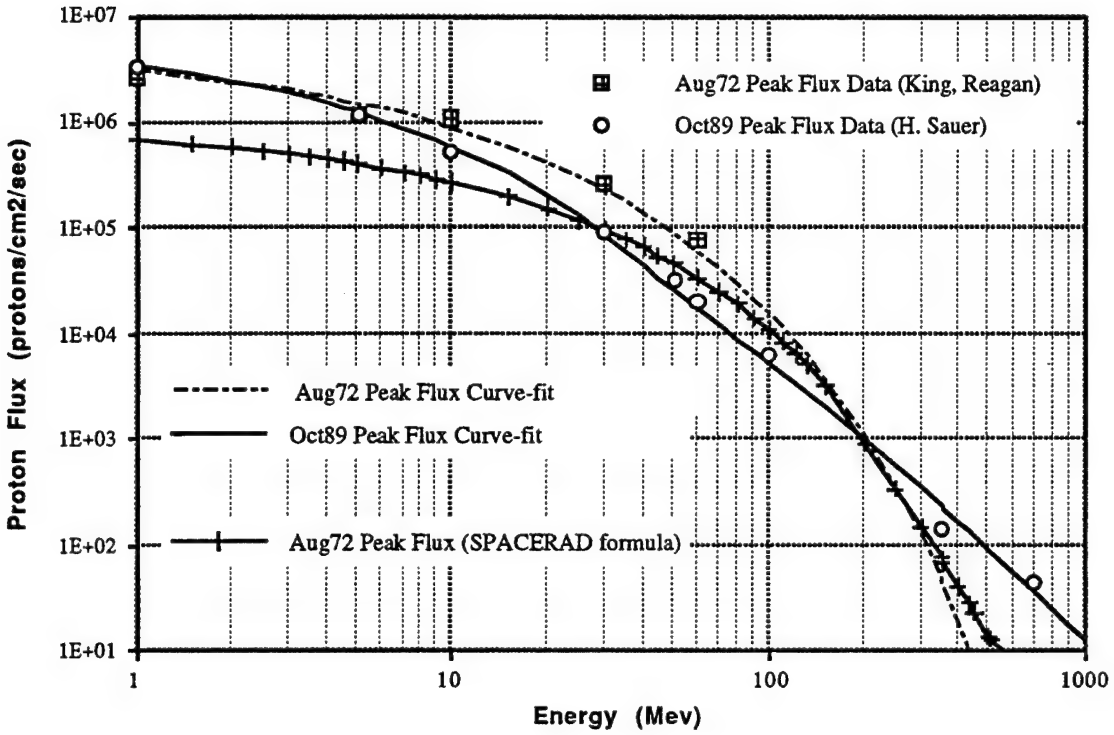

Figure 5. Peak Proton Integral Flux of Aug72 and Oct89 Solar Flare Events in Geosynchronous Orbits

Note that the Aug72 peak flux formula,[7] as implemented in the SPACERAD code, is for the differential flux. Equation (7), for integral flux, is derived from this peak formula by integration. The constant term in the first part of Eq. (6) has been added to ensure continuity of the expression at E=150 MeV.

From the peak flux description of the Aug72 and Oct89 events, a new worst-case composite flux model, referred to as Composite(Aug72,Oct89), has been derived. Figure 6 compares this model with the worst-case flux model implemented in the Cosmic Ray Effects on Micro

Electronics (CREME) code. The CREME model combines the Aug72 flare and the February 1956 (Feb56) flare; in Figure 6, the CREME curve below 150 MeV represents the Aug72 flare, and that above 150 MeV, the Feb56 flare. The proton flux of the CREME model exceeds that of the new model by 3 orders of magnitude in the energy region above 1000 MeV.

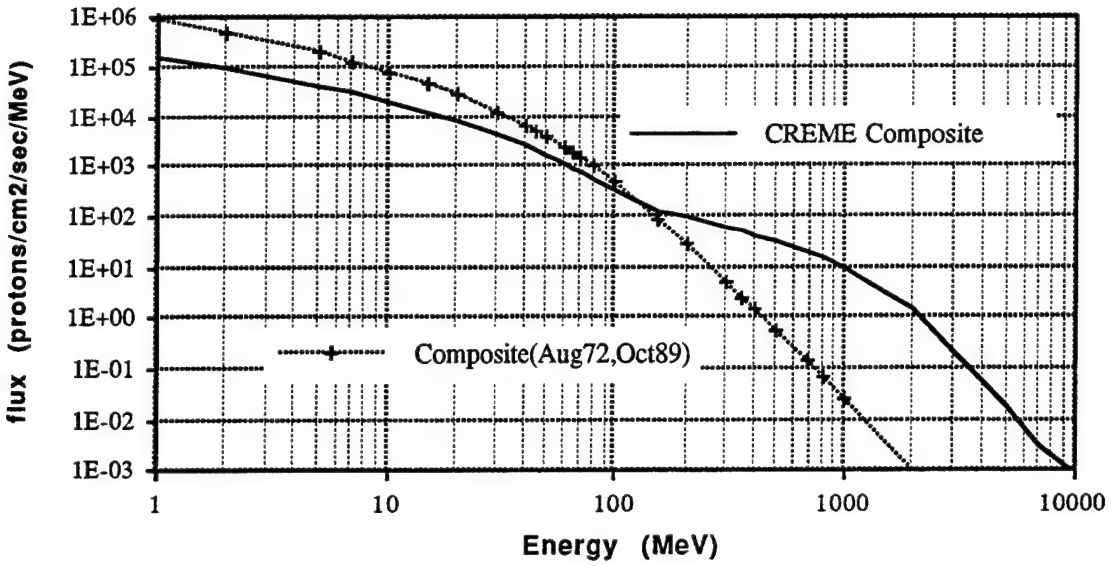

Figure 6. Peak Differential Proton Flux of Composite Worst-Case Flares in Geosynchronous Orbits per Composite(Aug72,Oct89) Model and CREME Composite Model

The proton differential fluxes of both composite models are expressed as follows, where the differential flux j is in units of protons/cm^2/sec/MeV, and the rigidity R_p is in MV:

(a) Composite(Aug72,Oct89) Model:

$$\begin{aligned} j &= 7.18\times10^4\left[dR_p/dE\right]exp(-R_p/75.8), \quad 1\le E\le 100\,MeV \\ &= 3.19\times10^{20}\left[dR_p/dE\right]R_p^{-6.86}, \quad E>100\,MeV \end{aligned} \tag{8}$$

(b) CREME Composite Model:

$$\begin{aligned} j &= 1.17\times10^4\left[dR_p/dE\right]exp(-R_p/100), \quad 1\le E\le 150\,MeV \\ &= 1.60\times10^2\left[dR_p/dE\right]exp(-R_p/580), \quad 150<E<3000\,MeV \\ &= 1.26\times10^{20}\left[dR_p/dE\right]R_p^{-5.8}, \quad E\ge 3000\,MeV \end{aligned} \tag{9}$$

Equation (9) for the CREME model is a numerically adapted version that is equivalent to the much more complex formula implemented in the CREME code.

3. Heavy-Ion Environment of Solar Flares

The heavy-ion environments described below have been derived from the proton spectra shown in Figures 3 and 5, using the CREME code procedures.[7] The derivation assumes that the ratio of the flux of any ion species to the proton flux is independent of energy value per nucleon, and that this ratio is equal to the mean solar abundance ratio relative to hydrogen, as given in Table 1. In Table 1, abundance ratios of elements other than those listed are less than 10^{-8}. Although these abundance ratios are omitted from the table, they are included in calculating the linear energy transfer (LET) spectra.

Table 1. Mean Abundance Ratio of Solar Flare Composition (first 30 elements) [a]

Atom Numb	Elem Symbol	Ratio	Atom Numb	Elem Symbol	Ratio	Atom Numb	Elem Symbol	Ratio
1	H	1.0	11	Na	3.2E-6	21	Sc	0
2	He	1.0E-2	12	Mg	6.4E-5	22	Ti	1.0E-7
3	Li	0	13	Al	3.5E-6	23	V	0
4	Be	0	14	Si	5.8E-5	24	Cr	5.7E-7
5	B	0	15	P	2.3E-7	25	Mn	4.2E-7
6	C	1.6E-4	16	S	8.0E-6	26	Fe	4.1E-5
7	N	3.8E-5	17	Cl	1.7E-7	27	Co	1.0E-7
8	O	3.2E-4	18	Ar	3.3E-6	28	Ni	2.2E-6
9	F	0	19	K	1.3E-7	29	Cu	2.0E-8
10	Ne	5.1E-5	20	Ca	3.2E-6	30	Zn	6.0E-8

[a]See Reference 7.

Figures 7 and 8 show the heavy ion environments associated with the Aug72 and Oct89 flares in geosynchronous orbits. In Figure 7, plots of the integral heavy-ion fluences shown as functions of LET have been derived from the proton fluence data in Figure 3. Similarly, the heavy-ion LET peak flux spectra shown in Figure 8 have been derived from the peak proton flux data in Figure 5.

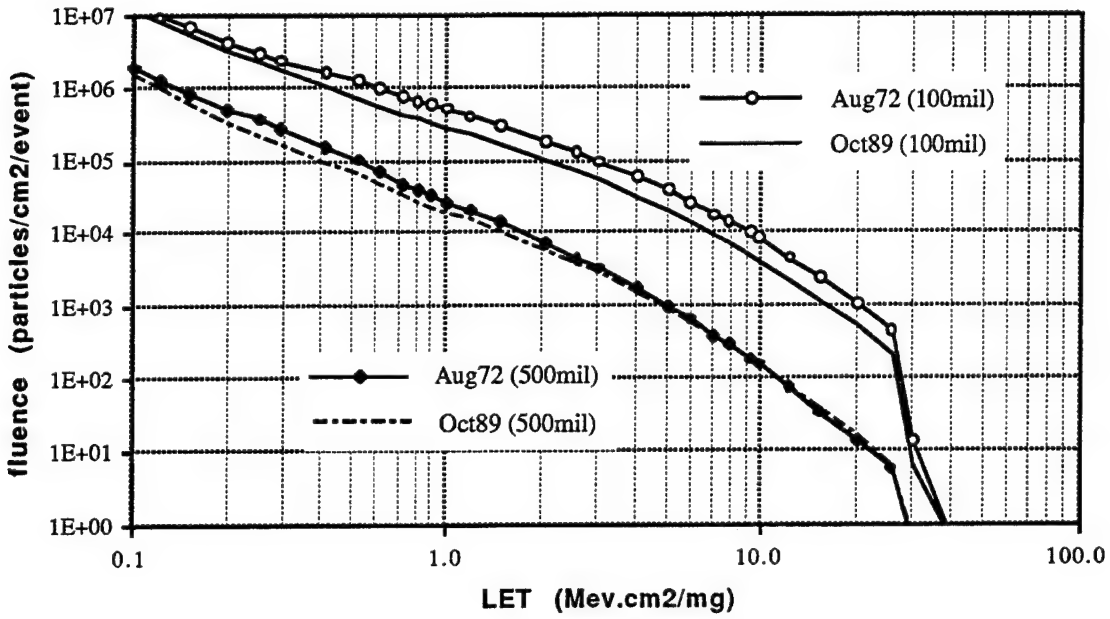

Figure 7. Integral Heavy-Ion Fluence of Aug72 and Oct89 Solar Flares in Geosynchronous Orbits Associated with Event Total Proton Fluence of Figure 3 (with aluminum shield of 100 and 500 mils)

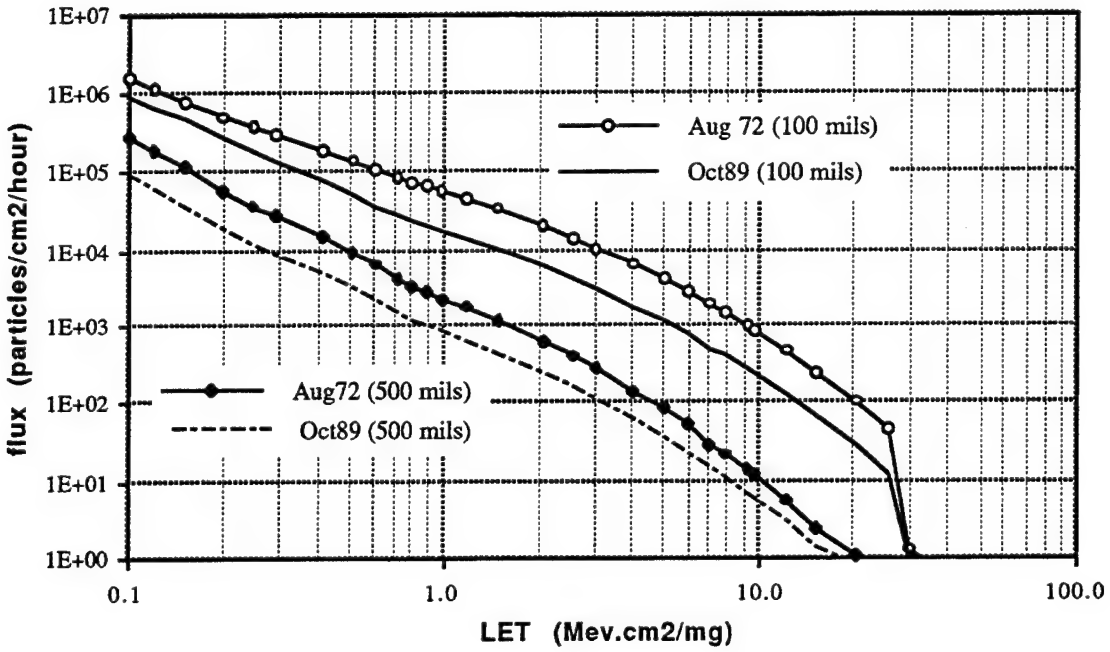

Figure 8. Peak Integral Heavy-Ion Flux of Aug72 and Oct89 Solar Flares in Geosynchronous Orbits Associated with Peak Proton Flux of Figure 5 (with aluminum shield of 100 and 500 mils)

Figure 9 exhibits the effectiveness of shielding in reducing SEUs caused solar flare heavy ions. In this figure, the event total SbSEUs of IDT 256K SRAM in a GEO during the solar flares are compared with each other and also with the annual SEU rate in the 90% worst-case, no-flare, heavy-ion environment. The SEU rate in the 90% worst-case environment decreases only by a factor of 3 when the shielding thickness increases from 100 to 2000 mils. On the other hand, in the solar flare environment, the number of SEUs drops an order of magnitude when the shielding thickness increases from 100 to 300 mils, and drops another order of magnitude from 300 to 900 mils; between 100 and 2000 mils, there is a drop of 3 orders of magnitude.

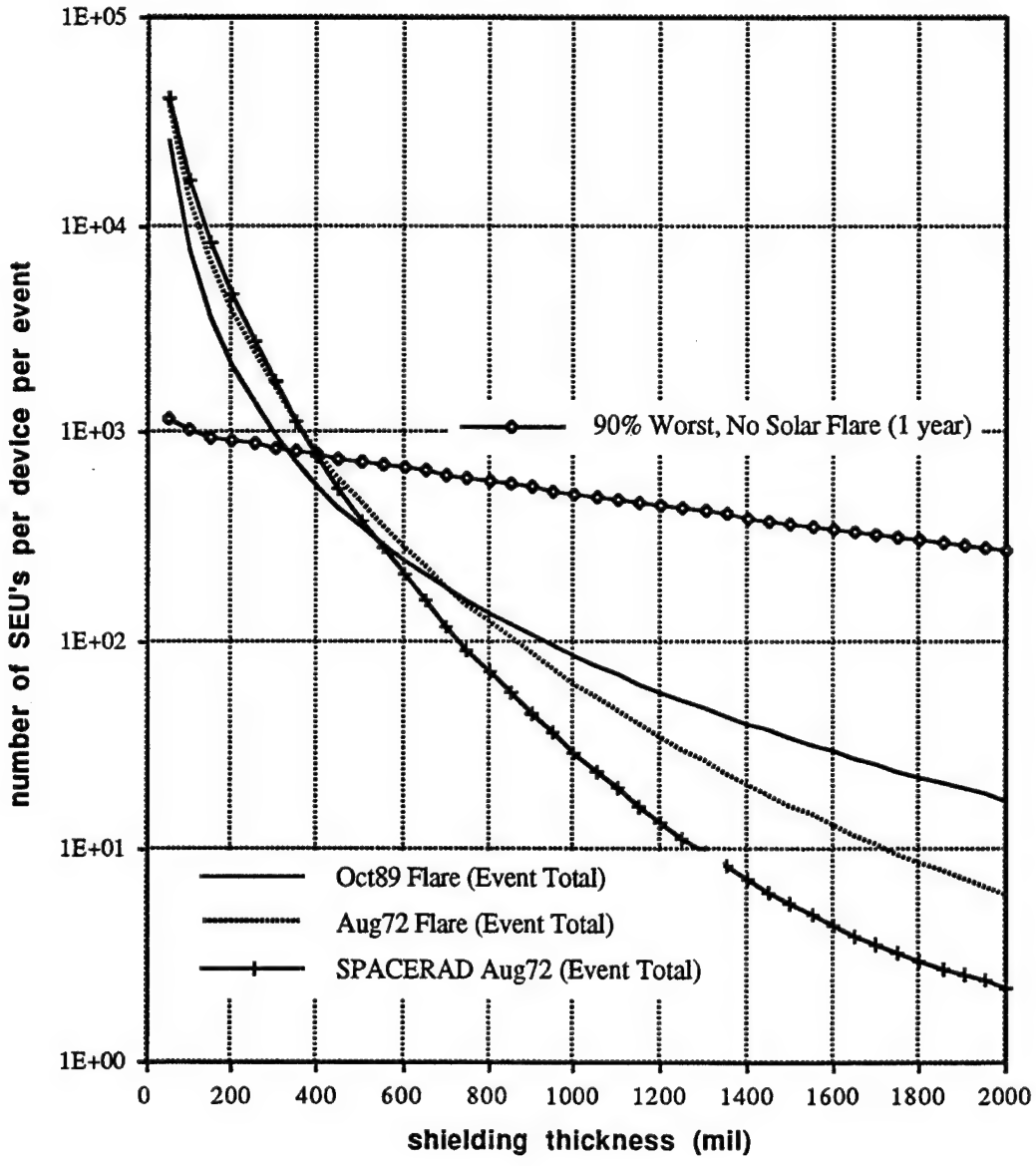

Figure 9. Event Total SEU of IDT 256K SRAM in Geosynchronous Orbits During Solar Flare (comparison with annual SEU rate in 90% worst-case, no-flare, heavy-ion environment)

Figure 10 shows the heavy-ion environments derived from the composite worst-case solar proton models of Figure 6; the new composite model, Composite(Aug72,Oct89), is compared with the CREME composite model.

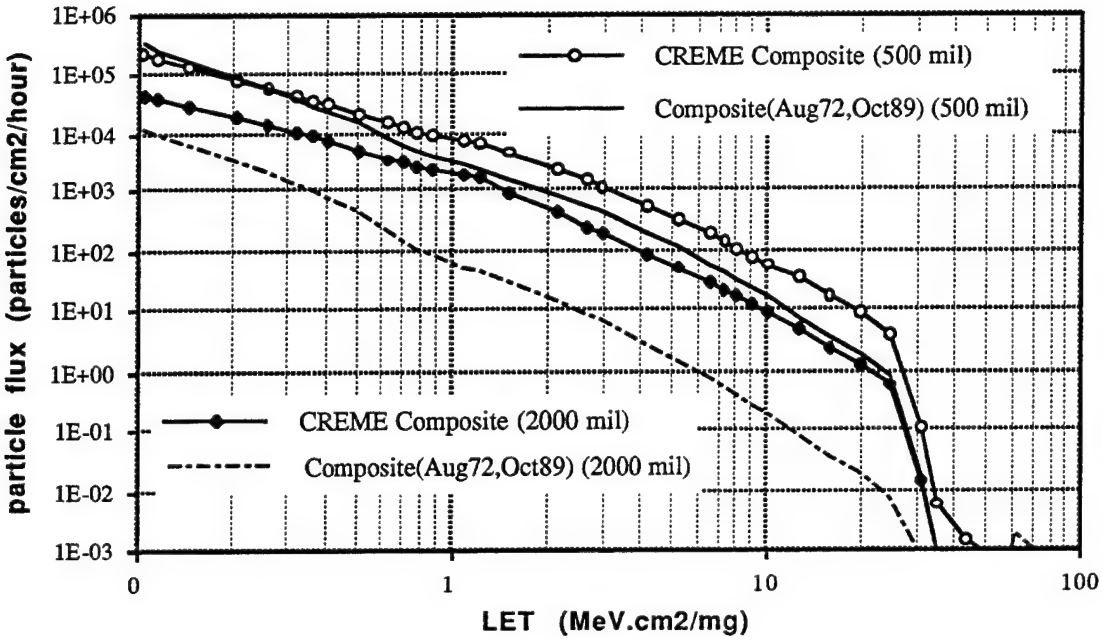

Figure 10. Peak Integral Heavy-ion Flux of Composite Worst-Case Solar Flares in Geosynchronous Orbits per Composite(Aug72,Oct89) Model and CREME Composite Model (with aluminum shield of 500 and 2000 mils)

The new composite model is comparable to the CREME model when the shielding thickness remains below 500 mils. The effect of the high proton flux of the CREME model in the energy region above 150 MeV (see Figure 6) becomes apparent as the shielding thickness approaches 500 mils. When the shielding thickness reaches 2000 mils, the difference between the two models is more than an order of magnitude. This difference is more clearly illustrated in Figure 11, where the heavy-ion environment is translated into an SbSEU rate in an IDT 256K SRAM device. The new model yields higher rates when the shielding thickness is less than 250 mils, and the rates of the both models stay comparable up to 500 mils. At the shielding thickness of 2000 mils, the CREME model's rate is higher than that of the new model by more than an order of magnitude.

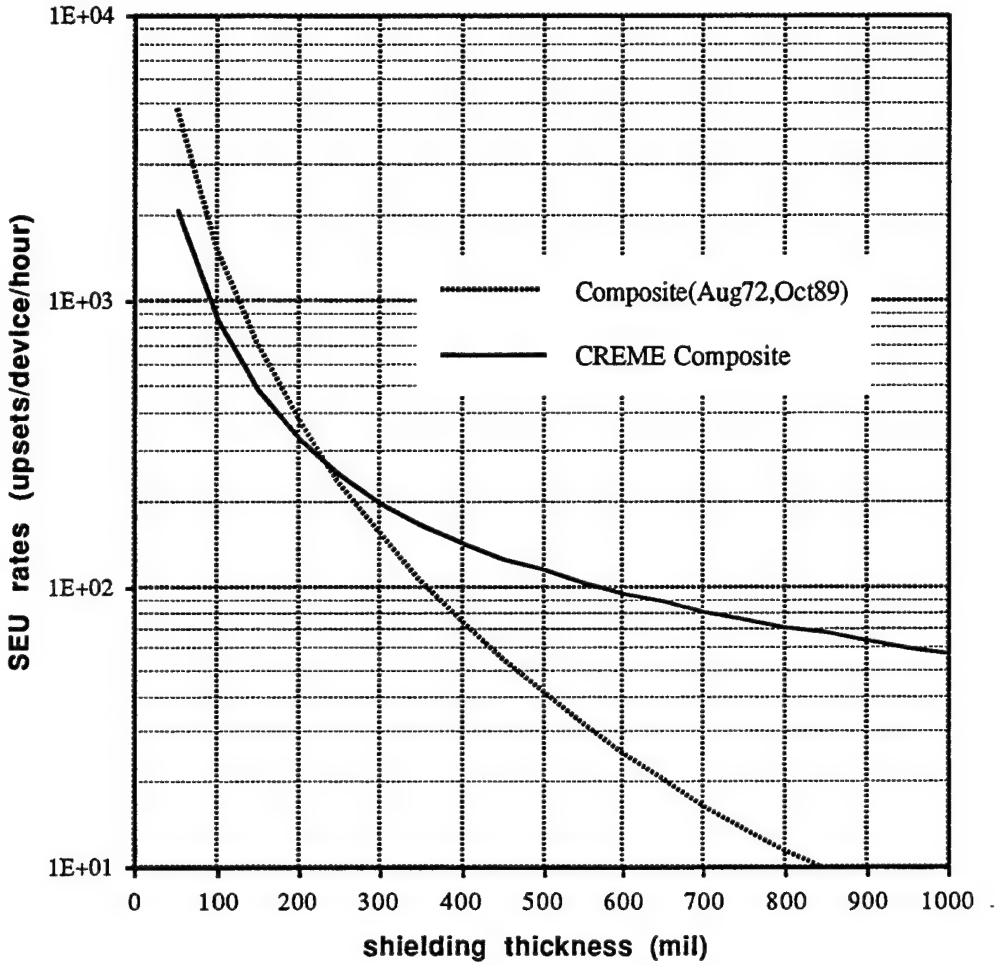

Figure 11. Hourly Single-bit SEU Rates of IDT 256K SRAM in Geosynchronous Orbits During Peak Hours of Composite Worst-Case Solar Flares [comparison of Composite(Aug72,Oct89) model and CREME composite model]

At this point, we should address the issue of the validity of assuming (1) that the spectra of all the heavy ion species have the same shape (as functions of energy per nucleon) as the proton spectrum, and (2) that the intensities relative to protons follow the corresponding solar abundance ratios. In an attempt to address this issue, Chenette and Dietrich examined data from 30 flares that occurred during the 1973–1983 solar cycle. [8] While generally there is agreement between the relative heavy ion flare and solar abundances, occasional enrichment relative to oxygen is noted for ions with atomic number >8. The differential heavy ion spectra discussed in Reference 8 have a power-law dependence on energy per nucleon, of the form:

$$\frac{dJ}{dE} = AE^{-\gamma} \qquad (10)$$

where J is the ion flux and E is the energy per nucleon. Values of the spectral index γ for oxygen range primarily between 2 and 5, with the midpoint of the distribution around 3.5. For the 24 September 1977 flare, the largest observed in the period, γ= 2.7 for both oxygen and iron.

Whenever the ratio of the energy per nucleon to the proton rest mass is small compared to 1, the spectral index δ in the power-law portions of integral flux given by Eqs. (2) and (6) can be related to γ in Eq. (10) by the expression

$$\gamma \approx \delta/2+1$$

For the total fluence of Eq. (2), we have γ=2.9, and for the peak flux case of Eq. (6), γ=3.3. Both values of γ lie in the middle of the distribution given in Reference 8. We therefore conclude that extrapolation of the proton spectral shape and intensity to heavy ions is reasonable, in the absence of heavy-ion data.

4. MbSEU Calculation for IDT 256K SRAM (IDT71256)

Multiple-bit single event upsets (MbSEUs) occur when an incident heavy ion penetrates through two or more neighboring bits belonging to the same word. Unlike single-bit single event upsets (SbSEUs), MbSEUs cannot be eliminated by single-error correction double-error detection (SECDED) techniques. Therefore, even though the probability of MbSEUs is much smaller than that of SbSEUs, the former is a primary concern, particularly when a large solar flare is in progress.

Figure 12 shows the relative geometry of two of the closest bit-cells in a single word of the IDT 256K SRAM used on the Titan/Centaur INU.[2] In the SRAM layout, these two cells are separated by 15 other cells, each belonging to a different word. Figure 12 lists the overall dimensions of the cells and and of the SEU-sensitive volume within the cells, together with the critical charge (Qc) for SEU.

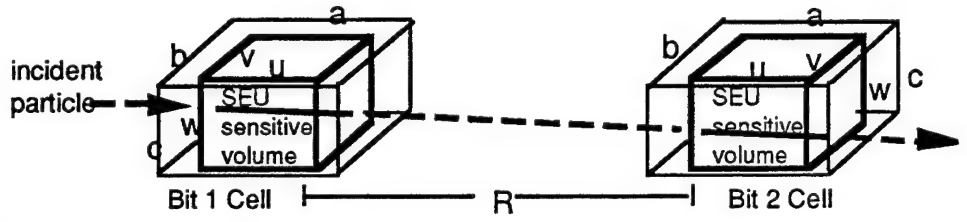

a=9.7μm, b=11μm, c=2.5μm; u=4μm, v=6μm, w=2.5μm; R=151.2μm; Qc=70fC

Figure 12. Properties of Two Neighboring Bit-Cells in a Single Word of an IDT 256K RAM

The MbSEU rates for the IDT 256K SRAM were computed using the Aerospace MULTSEU code.[10] In addition, the commercially available SPACERAD code was used to compute the SbSEU rates. The SbSEU rates are compared with the MbSEU rates in Figure 13.

All present calculations assume a particle environment in the Titan/Centaur GSO transfer orbit during peak hours of the Aug72 and Oct89 events, as shown in Figure 8. The transfer orbit is specified by the axes of a 96.2 × 19,412.5 nmi altitude and a 26.6° inclination. Other relevant parameters used in the calculations are listed in Figure 12.

Figure 13 shows the results of the calculations for an SbSEU and an MbSEU as functions of aluminum shielding thickness. Also shown for comparison is the result of a previous MbSEU rate calculation,[2] which assumed an omnidirectional shielding thickness of 100 mils of aluminum. Note that for the SbSEU, the ordinate units in Figure 13 are the number of upset *bits* per hour per device, while for the MbSEU, the units are the number of upset *words* per hour per device.

Figure 13 indicates that the ratio of MbSEU to SbSEU is approximately 10^{-4}, a value that should reflect the ratio of the solid angles subtended by the "detectors" of the respective types of SEU. From Figure 12, it is easy to deduce that these solid angles are, respectively, $2(vw/R^2)$ and 4π. Therefore, the ratio = $vw/2\pi R^2 = 6 \times 2.5/(2\pi \times 151.2^{2)} = 1.04 \times 10^{-4}$, in excellent agreement with the results of Figure 13.

The trends in the data of Figure 13 directly reflect the nature of the heavy-ion environments shown in Figure 8. In the case of no shielding, the Aug72 peak heavy ion flux is about 1.5 times the Oct89 flux. This trend is reflected by the ratio of upset rates at zero shielding thickness, shown in Figure 13. As the shielding thickness increases, the heavy-ion flux ratio increases up to about 3, which is reflected in the SEU rates of Figure 13.

Figure 13 confirms the preceding qualitative conclusion, made on the basis of Figure 9, that aluminum shielding is quite effective in reducing solar flare SEUs. The silicon material of the microelectronic chips provides practically the same shielding effectiveness as aluminum. The effectiveness of the silicon material, and the fact that shielding against MbSEUs matters only in the lateral grazing angle direction, implies that the inherent shielding around the memory chips can be very effective in reducing MbSEU vulnerability. This implication has already been pointed out in terms of "self-shielding" in the previous Aerospace work, where the MbSEU rate calculation considered only a 100 mil spherical shield. [2]

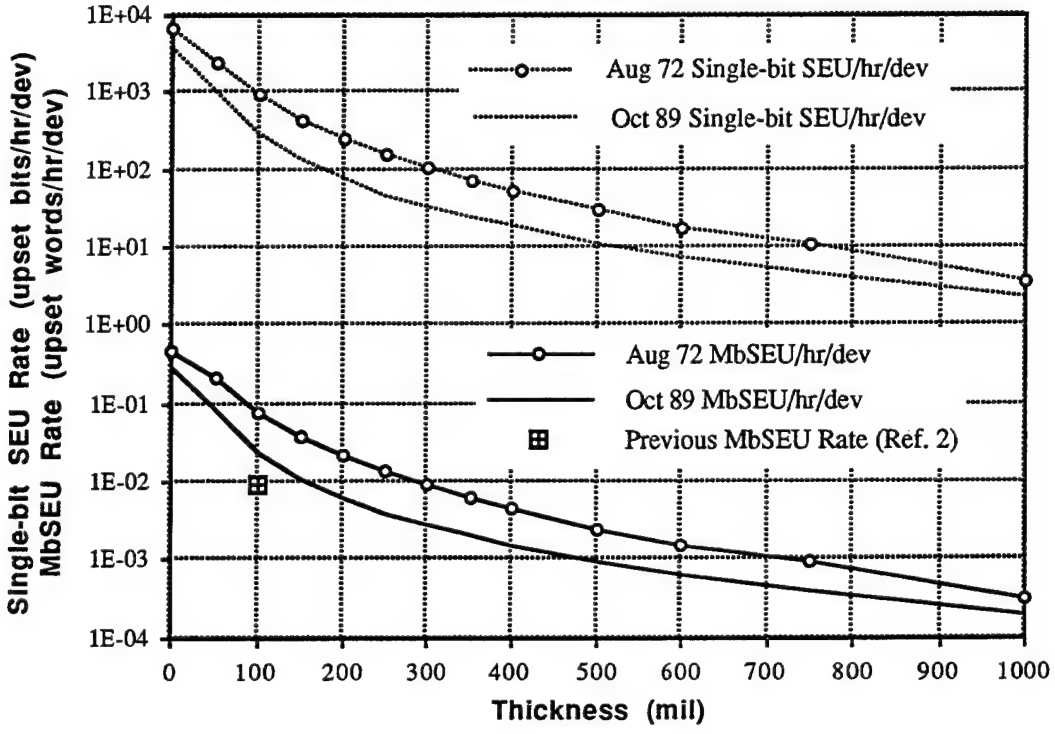

Figure 13. Single-bit and Multiple-bit SEU Rates During Peak Solar Flare Hours (at 96.2 × 19,412.5 nmi 26.6° Titan/Centaur GSO transfer orbit)

5. MbSEU Calculation for Titan/Centaur INU

Titan/Centaur employs 24 chips of the IDT 256K SRAMs for the inertial navigation unit (INU). The chips are mounted in six packages, four per package. Three packages are located on the inertial measurement subsystem-processor (IMSP) board, and three packages on the flight control subsystem-processor (FCSP) board. Of the total memory, 48% is used to store the navigation instructions. The mission flight time is approximately 6 hours. The SbSEUs are corrected by SECDED logic.

Figures 14a through 14e display geometrical configurations of the INU memory boards. Figure 14a shows the dimensions of the SRAM integrated circuit (IC) package. Figures 14b and 14c illustrate the device package arrangement on the PCBs for IMSP and FCSP, respectively. The three memory packages are circled. Figure 14d locates the boards in the INU box, together with the low voltage power supply (LVPS), positioned on the right-hand side of the boards. LVPS provides a minimum of 300 mils aluminum-equivalent shielding. Figure 14e is a perspective view of the INU. Since the INU box is mounted on the launch-vehicle body, particle penetration from the bottom side of the box can be neglected. For MbSEU, the memory package itself provides significant shielding for the memory cells, as do all the neighboring packages on the same board.

A new computer code, MbSEU_PCB, was developed to take into account the anisotropic shielding geometry of the PCBs. The code reads in the input data describing the geometrical configurations surrounding the memory-bit pair in question, and calculates the effective shielding thickness in each particle-beam direction. The CREME code was revised to yield an output file of particle flux for various shielding thicknesses, so that, via interpolation of thickness, the number of upsets could be calculated for each particle-beam direction. [7]

Table 2. INU's MbSEU Survival Probability During Peak Hours of Solar Flare Events (in 96.2 × 19,412.5 nmi 26.6° Titan/Centaur GSO transfer orbit)

Solar Flare Size	MbSEU Rate (per hr)	MTBF (hr)	Survival Probability
Aug72	3.24E-3	309	0.98077
Average-sized	1.54E-5	64,884	0.99991
Three-times Average	3.57E-5	28,011	0.99979

Table 2 lists the computation results of the MbSEU_PCB code for three different solar flare events during Tital/Centaur's GSO transfer mission: the Aug72 event, an average-sized flare

event, and a three-times average-sized flare event. The second column in Table 2 indicates the MbSEU rates per hour for INU, the third column is the INU mean time between failures (MTBF), and the fourth column is the MbSEU survival probability for the 6-hour mission. The definition of the average solar flare in terms of the proton fluence spectrum is provided in Appendix B.

The three-times average-sized flare event was chosen to indicate roughly the maximum flare size for which the INU meets the SEU requirement of 25,000 hours MTBF. As indicated in the Introduction, average-sized flares occur about 3.4 times per solar-active year, while a three-times average-sized event is seen about twice per active year.

For the Titan/Centaur launch operation, the current GO/NO-GO criterion stipulates that the launch be aborted whenever the proton flux equals or exceeds 10 pfu of proton energy greater than 50 MeV [1 particle flux unit (pfu) means 1 particle/cm^2/sec/steradian]. This is the particle environment during the peak hours of an average-sized solar flare (see Figure B-3, Appendix B). Since the SEU MTBF requirement of 25,000 hours is met even during a three-times average-sized flare, the criterion can be relaxed from 10 to 30 pfu. This relaxation increases the available launch-time window. With the assumption that, on the average, 7 days are removed from the window for each solar flare event, the 10 pfu threshold results in an average loss of 24 days per year, whereas the 30 pfu threshold results in an average loss of 14 days per year.

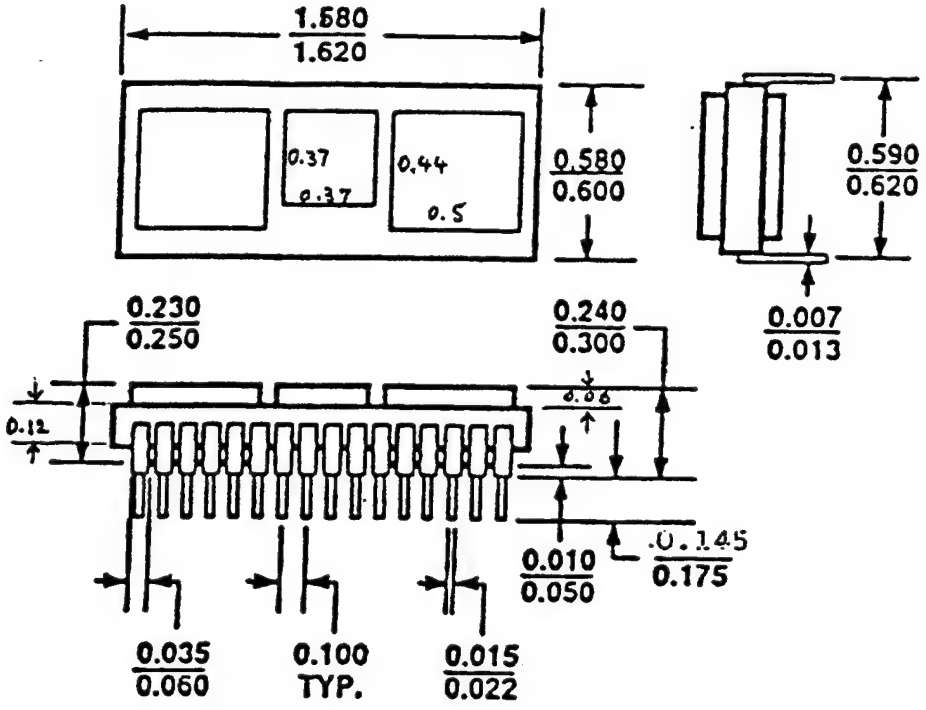

Figure 14a. INUs IDT 256K SRAM Package

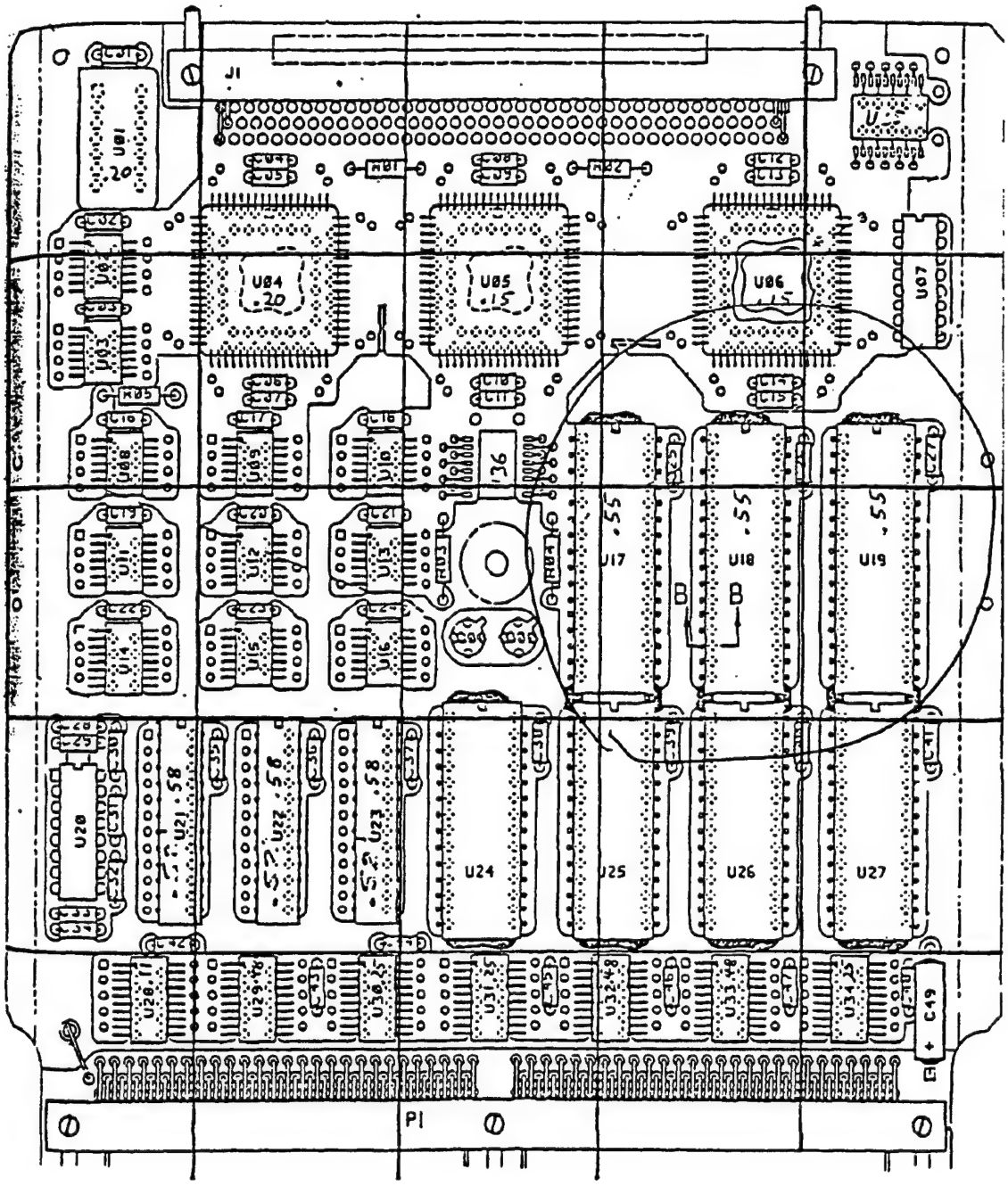

Figure 14b. INU IMSP Board

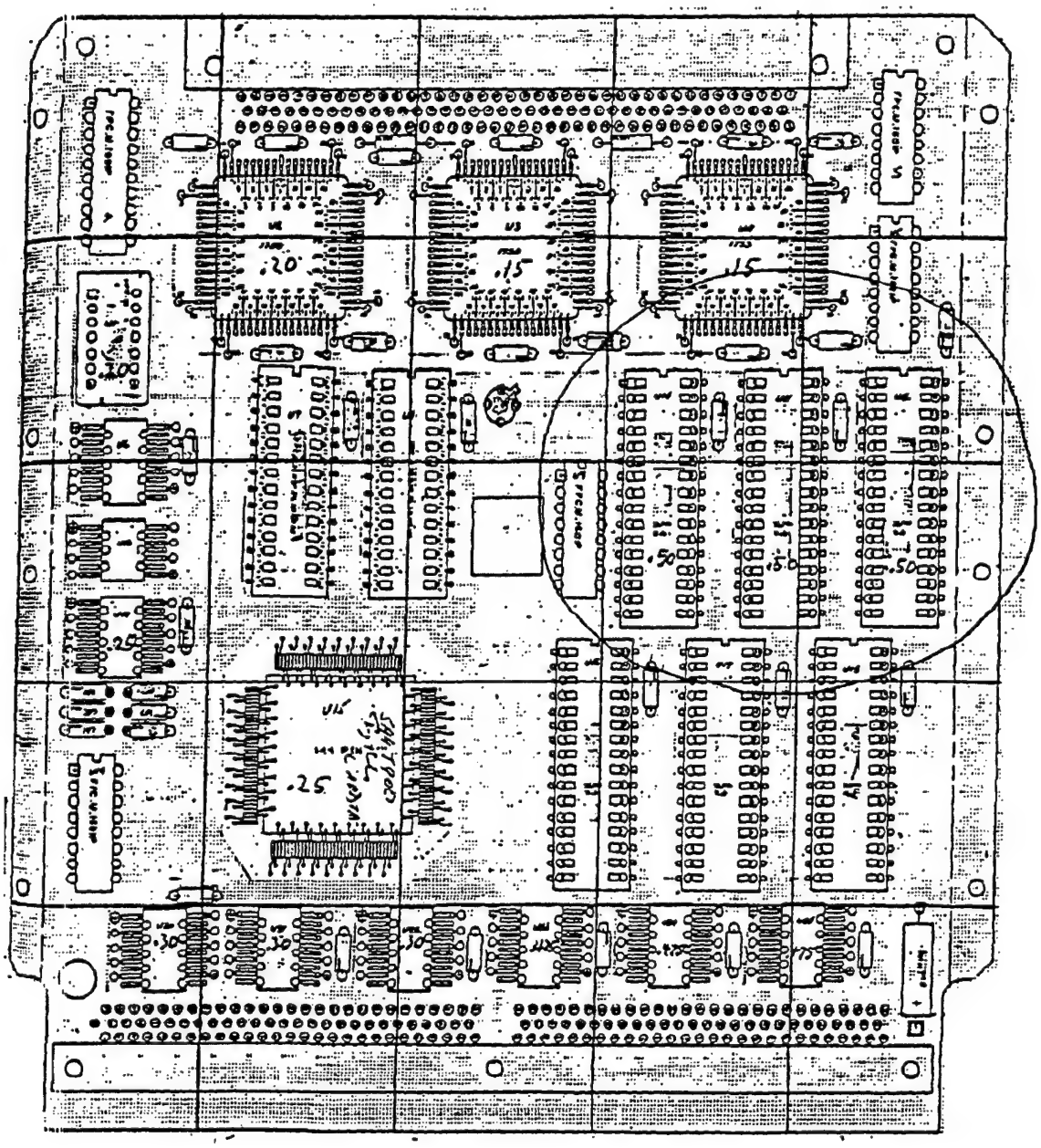

Figure 14c. INU FCSP Board

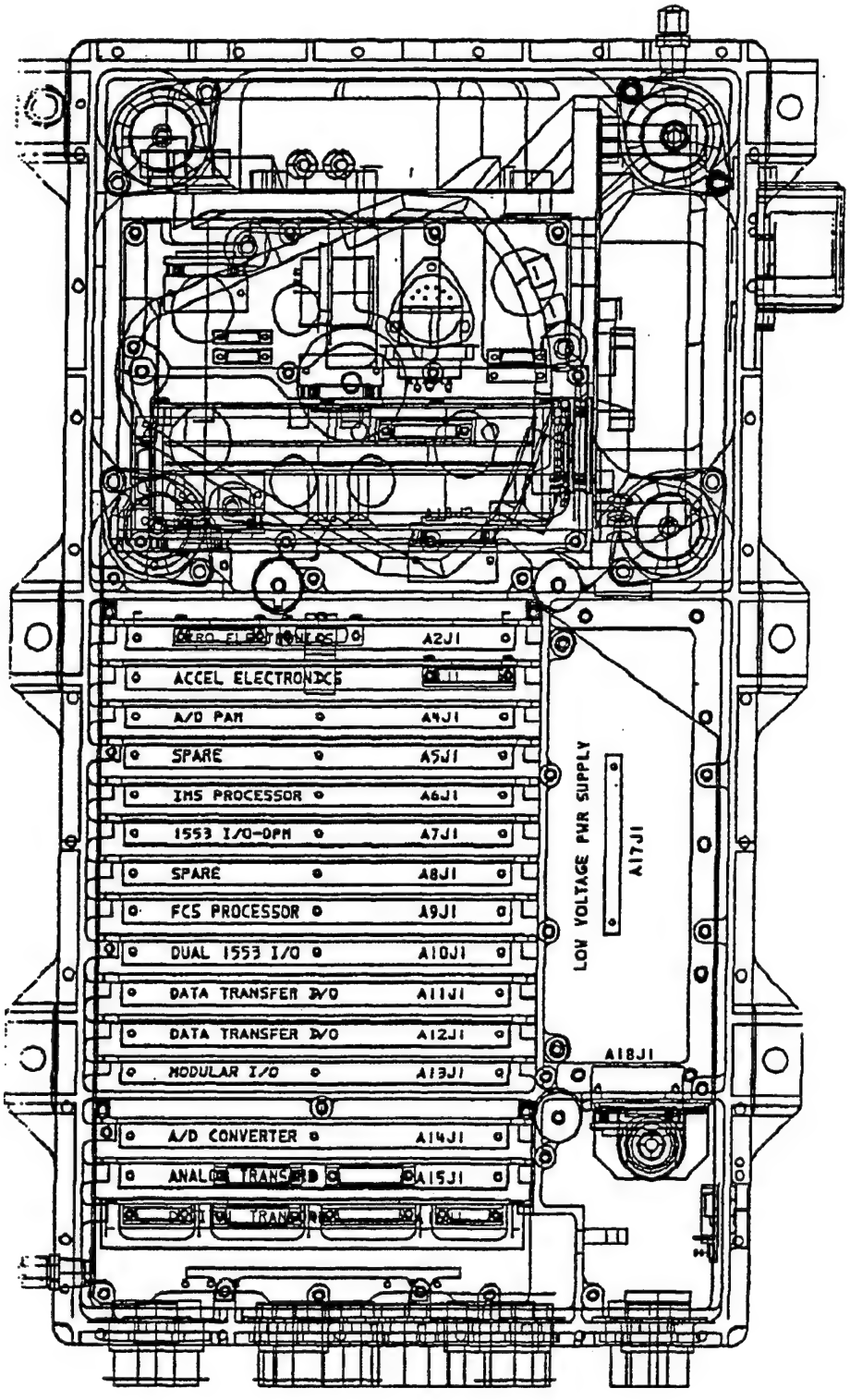

Figure 14d. INU Top View

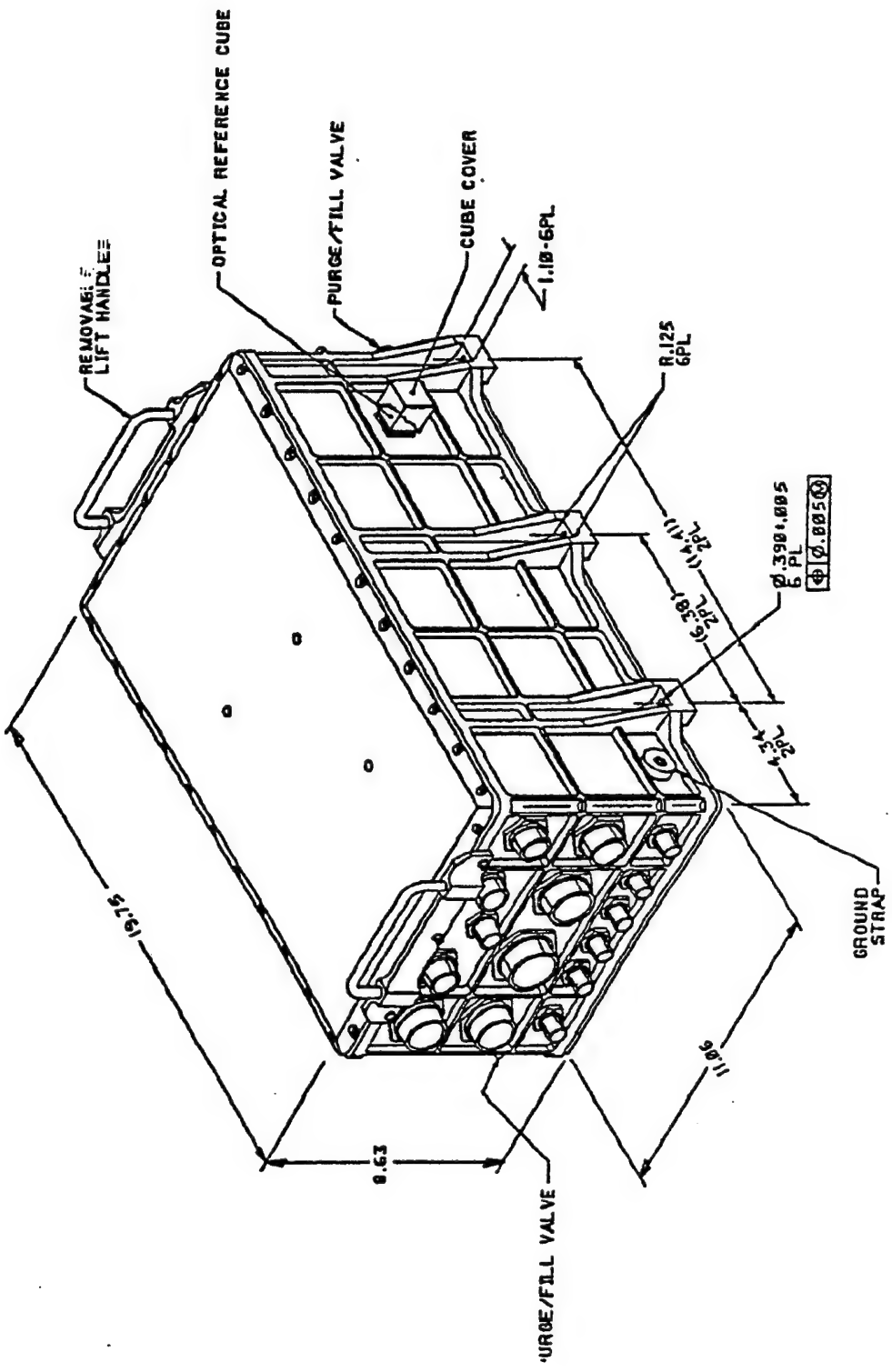

Figure 14e. INU Perspective View

6. Summary and Conclusions

In summary, we have used data from the National Oceanic and Atmospheric Administration (NOAA) and from Lockheed to augment the existing model of the Aug72 solar flare event, generate a model for the Oct89 solar flare, and, by combining the data, formulate a composite, worst-case solar flare model. We have also defined the particle environment corresponding to an average solar flare event based on the NOAA data set. As an application of these models, we calculated the multiple-bit single event upset (MbSEU) rates in the Titan/Centaur inertial navigation unit (INU) during the peak hours of the Aug72 and Oct89 events, as well as of an average solar flare event. A new computer code, MbSEU_PCB, was developed for these calculations, to take into account the anisotropic shielding provided by the INU printed circuit boards (PCBs) where the memory chips are located.

The MbSEU study of the INU refers to the 6-hour geosynchronous orbit (GSO) transfer mission of the Titan/Centaur launch vehicle in an orbit with 26.6° inclination. The study leads to the following conclusions:

1. Shielding by aluminum walls and integrated circuit (IC) packages on the PCB is very effective in reducing the MbSEU rate during solar flares. This shielding is effective because, for MbSEU, it is needed only in the lateral direction over a small range of grazing angles. The inherent shielding in this direction can readily exceed the equivalent of 1000 mils of aluminum when all the neighboring devices and structures in the same PCB plane of the memory chip are taken into account. For the Titan/Centaur GSO transfer mission, the predicted mean time between failures (MTBF) of the INU is about 300 hours during the peak hours of the Aug72 event, in contrast to the previously calculated result of a 10-hour MTBF for an isotropic 100 mil aluminum-equivalent shielding distribution. [2]

2. The average solar flare yields a flux of 10 pfu with proton energies greater than 50 MeV [1 particle flux unit (pfu) means 1 particle/cm^2/sec/steradian]. The MTBF for the INU, resulting from MbSEU during the peak hours of the average event, is calculated to be about 65,000 hours. For a three-times average flare, the MTBF is about 28,000 hours, which exceeds the present 25,000 hour requirement. Consequently, the present GO/NO-GO threshold of 10 pfu for the Titan/Centaur launch operation can be relaxed to 30 pfu. Solar flares larger than the average flare occur 3.4 times per solar-active year, while those larger than the three-times average flare occur two times. Thus, the relaxation from 10 pfu to 30 pfu allows a wider launch-time window.

Appendix A: Probability of Solar Flare Events

Very large solar flares, such as the Aug72 and Oct89 events, pose serious threats to spacecraft systems. However, since such solar flares are rare, it is practical to establish how likely one is to be encountered during a particular mission. This issue has been recently addressed by Feynman, Spitale, and Wang, who analyzed the 30-year solar flare proton fluence data of the period between 1963 and 1991.[3] They found that the probability of solar flare occurrence is bimodal, in the sense that it is nonzero during 7 active years out of the 11-year solar cycle, and negligible otherwise. They also found that the probability of proton fluence exceeding a given level in an event during the solar active years is well represented by the lognormal distribution function.

Let the fluence F_E in units of protons/cm^2/event be a proton fluence of energy greater than E MeV. Then, the lognormal distribution is given by the following expression:

$$Prob(F_E) = probability\ that\ the\ fluence\ of\ protons\ with\ energies > E\ exceeds\ F_E$$

$$= \frac{1}{\sqrt{2\pi}\sigma_E} \int_{F_E}^{\infty} \exp\left\{-\frac{[\ln(f/\mu_E)]^2}{2\sigma_E^2}\right\} d[\ln(f)]$$

The parameters μ_E and σ_E, respectively, denote the mean fluence and the standard deviation; they are functions of energy E. The results of the Feynman, Spitale, and Wang data analysis are summarized in Table A-1,[3] and the lognormal plots for proton energies greater than 1, 10, and 30 MeV are shown in Figure A-1. Note that σ_E is the standard deviation of *ln*(fluence), instead of *log*(fluence).

Table A-1. Statistics of Solar Flares During 1963–1991[a]

Energy E	Mean Fluence μ_E (prot/cm^2/event)	Std Deviation σ_E of *ln*(fluence)	Years of Observation	Total Number of Flares
> 1 MeV	3.0E+09	1.40	10.6	89
> 4 MeV	1.3E+08	2.21	10.6	122
> 10 MeV	7.3E+07	2.23	16.9	114
> 30 MeV	1.0E+07	2.53	16.9	122
> 60 MeV	8.0E+06	2.46	16.9	80

[a]See Reference 3.

If we choose to study the proton fluence of energy greater than 10 MeV, the mean fluence is μ_E=7.3E+07 protons/cm^2/event (Table A-1), and the probability for an event total proton fluence to exceed this fluence is 50% (Figure A-1), confirming that the fluence 7.3E+07 is

indeed the mean fluence. Thus, the average-sized solar flare can be characterized by the magnitude of the event total proton fluence of 7.3E+07 protons/cm^2/event of proton energies greater than 10 MeV. Table A-1 also shows that, during 16.9 solar-active years of observation, there were 114 solar flares: 50% (57 flares) below the average-sized flare, and 50% above the average-sized flare. This means that the above-average-sized solar flares occur at a rate of 3.4 times per year, in a solar-active year.

Continuing with protons of energies greater than 10 MeV, Figure A-1 indicates that the probability for a fluence greater than 1E+10 protons/cm^2/event (i.e., one like the fluence magnitude of the Aug72 or Oct89 flare) is 1.3%. Hence, the expected number of solar flares exceeding this fluence level out of 114 flares in 16.9 years is:

=0.013x114 events in 16.9 active years

=1.48 events in 16.9 active years.

This means that very large solar flares, such as that of the Aug72 or Oct89 event, occur at the rate of 0.088 flares per active year, i.e., once in 11 active years. Since there are 7 active years in every 11-year solar cycle, the occurrence rate is once in about 17 calendar years.

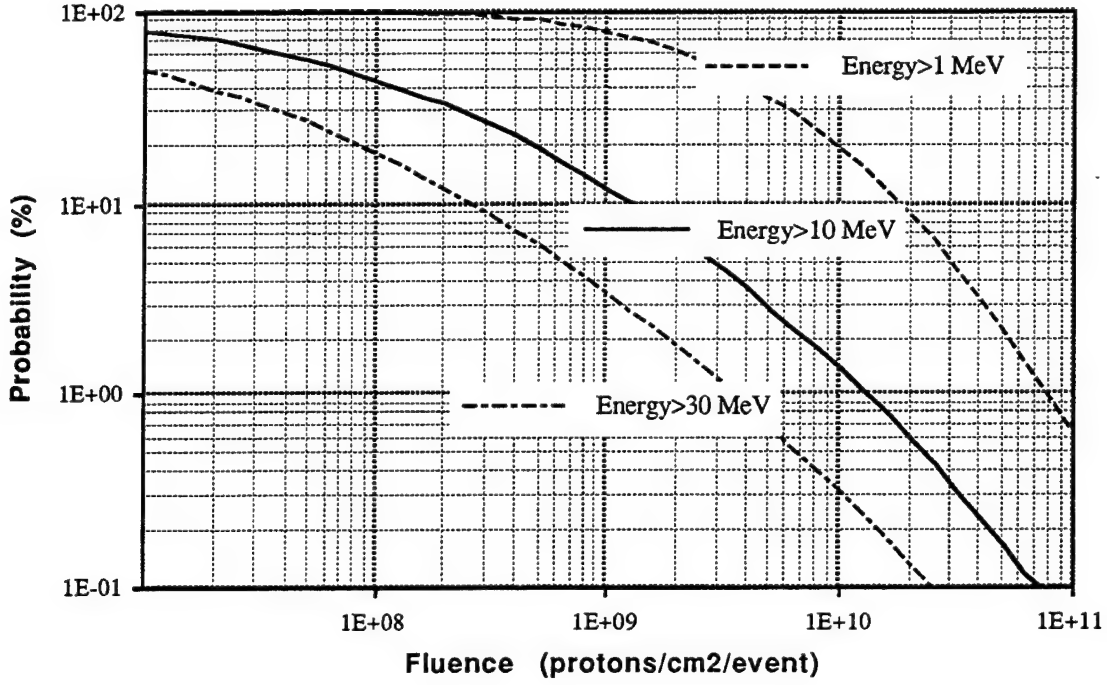

Figure A-1. Probabilities of Solar Flare Proton Fluence of Energies Greater than 1, 10, and 30 MeV

Appendix B: Definition of the Average Solar Flare

The 30-year solar flare statistical data in Reference 3, as summarized in Appendix A, do not contain sufficient information to provide a working definition of an average solar flare event. Such a definition would be useful for predicting SEU rates. The information is insufficient because the energy spectrum of an average flare of Reference 3 stops at 60 MeV, and because no data about peak flux magnitude are provided.

To remedy this situation, solar flare data of References 4 and 11, covering 13 events during the 4 years between December 1988 and June 1992, were searched and analyzed. Table B-1 shows the event total proton fluences of the 13 solar flares in the 4-year period covered by Reference 4. The average fluence for the period is shown in the bottom row of Table B-1. Note that this average is not the same as that for the 30-year period discussed in Appendix A.

Table B-1. Event Total Proton Fluence of Solar Flares of December 1988 to June 1992 [a]

Solar Flares	Event Total Proton Fluence of Solar Flares (protons/cm^2) for Energies (MeV) Greater Than							
	1.0	5.0	10.0	30.0	60.0	100.0	355.0	685.0
Dec 88	1.10E+09	6.43E+07	2.15E+07	8.52E+06	4.56E+06	2.30E+06	1.84E+05	1.11E+05
May 89	1.61E+09	9.97e+07	2.65E+07	5.96E+06	2.90E+06	1.40E+06	1.53E+05	1.22E+05
Jul 89	5.54E+07	2.22E+07	1.64E+07	8.11E+06	3.83E+06	1.82E+06	1.48E+05	8.31E+04
Aug 89	3.15E+10	1.30E+10	7.86E+09	1.52E+09	2.11E+08	4.55E+07	2.00E+06	6.17E+05
Sep 89	1.01E+10	5.54E+09	3.85E+09	1.42E+09	4.87E+08	1.90E+08	1.12E+07	4.68E+06
Oct 89	1.03E+11	3.90E+10	1.93E+10	4.24E+09	1.21E+09	4.60E+08	2.64E+07	7.92E+06
Nov 89	5.46E+08	3.54E+07	1.61E+07	5.70E+06	2.56E+06	1.19E+06	2.54E+05	2.09E+05
Dec 89	1.55E+10	5.66E+09	2.15E+09	1.30E+08	6.21E+06	5.09E+05	1.77E+05	1.22E+05
May 90	2.50E+09	6.43E+08	3.61E+08	1.39E+08	6.01E+07	2.84E+07	2.18E+06	9.85E+05
Mar 91	4.43E+10	1.69E+10	9.80E+09	1.81E+09	1.66E+08	1.74E+07	5.89E+05	8.77E+04
May 91	1.44E+09	3.25E+08	1.38E+08	1.82E+07	3.72E+06	1.16E+06	4.41E+04	2.82E+04
Jun 91	1.93E+10	4.88E+09	2.57E+09	6.27E+08	1.57E+08	4.98E+07	1.92E+06	6.99E+05
Jun 92	1.50E+09	5.24E+08	2.85E+08	4.74E+07	9.43E+06	3.03E+06	1.43E+05	7.88E+04
Average Fluence	4.20E+09	9.75E+08	4.78E+08	1.11E+08	2.76E+07	8.51E+06	6.13E+05	2.87E+05

[a]See Reference 4.

The peak-hour proton flux data corresponding to Table B-1 are given by Reference 11. The data are summarized in Table B-2, where the blank cells in the 355 and 685 MeV rows

indicate that no data are available in Reference 11, except for the Oct89, May90, and Jun91 events, with data from Reference 4.

Table B-2. Peak-Hour Proton Flux of Solar Flares of December 1988 to June 1992[a]

Solar Flares	Peak-Hour Proton Flux of Solar Flares (protons/cm²/sec/str) for Energies (MeV) Greater Than							
	1.0	5.0	10.0	30.0	60.0	100.0	355.0	685.0
Dec 88	1.27E+02	3.40E+01	4.40E+00	2.60E+00	2.60E+00	1.40E+00		
May 89	5.67E+03	1.24E+02	7.10E+00	1.10E+00	1.00E+00	6.00E-01		
Jul 89	5.14E+02	2.37E+01	1.98E+01	1.95E+01	1.42E+01	6.90E+00		
Aug 89	4.12E+04	6.07E+03	3.47E+03	1.22E+03	2.72E+02	5.50E+01		
Sep 89	6.92E+03	3.94E+03	2.78E+03	1.12E+03	6.87E+02	2.98E+02		
Oct 89	2.79E+05	9.26E+04	4.12E+04	7.44E+03	1.64E+03	4.94E+02	2.60E+01	1.00E+01
Nov 89	2.15E+02	2.80E+01	1.77E+01	1.40E+01	1.03E+01	4.90E+00		
Dec 89	2.08E+04	8.00E+03	1.71E+03	1.42E+02	1.30E+01	1.00E+00		
May 90	4.20E+03	6.83E+02	3.52E+02	1.09E+02	3.90E+01	1.80E+01	1.80E+00	1.00E+00
Mar 91	2.64E+05	6.75E+04	2.09E+04	6.01E+03	1.03E+03	9.00E+01		
May 91	1.87E+03	5.04E+02	1.28E+02	3.30E+01	1.70E+01	6.00E+00		
Jun 91	1.45E+04	4.15E+03	2.83E+03	7.20E+02	1.64E+02	6.60E+01	4.00E+00	2.00E+00
Jun 92	1.55E+03	3.62E+02	1.30E+02	3.70E+01	2.30E+01	1.10E+01		
Average Flux	5.66E+03	1.04E+03	3.72E+02	1.15E+02	4.58E+01	1.48E+01		

[a]See Reference 11.

Tables B-1 and B-2 show that the May 1990 (May90) event represents quite well the average for the 4-year data. The May90 event total integral fluence at 10 MeV is 3.61E+08 protons/cm^2 (see Table B-1), which is about five times that of the 30-year average of 7.3E+07 protons/cm^2 (see Table A-1).

Thus, for calculating SEU rates, the average solar flare event is defined by scaling down the May90 event by a factor of 5, both for the event total fluence and the peak-hour flux.

Figure B-1 shows the proton flux observed during the first 12 days of the May90 event between May 20 and June 3, 1990. The flux actually appears as a composite of four solar flares.[4]

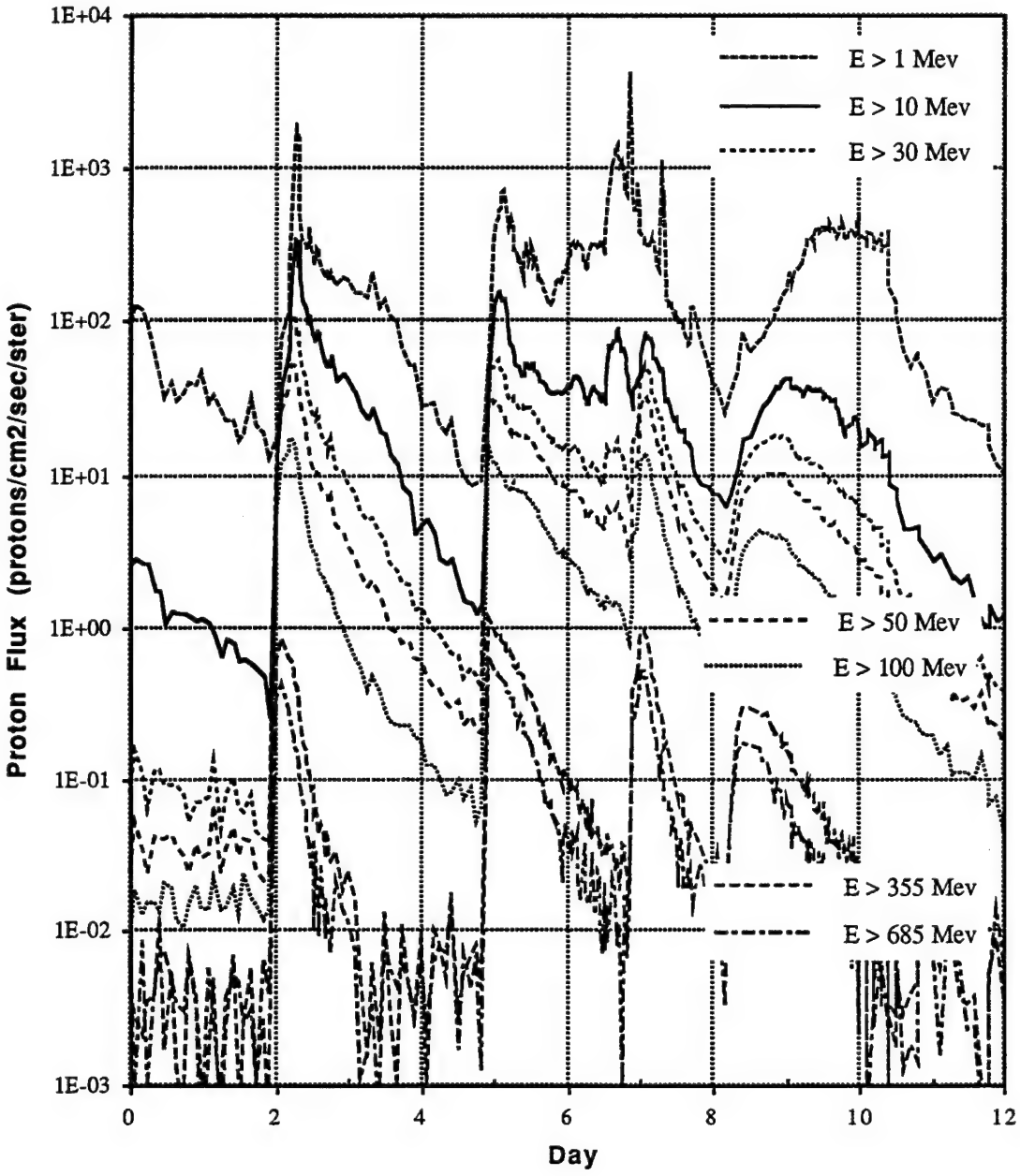

Figure B-1. Proton Fluence of First 12 Days of May90 Event

Figures B-2 and B-3 show, respectively, the event-total integral fluence and peak integral flux of the May90 event, as well as of the average events. Note that the peak flux unit is per steradian (str).

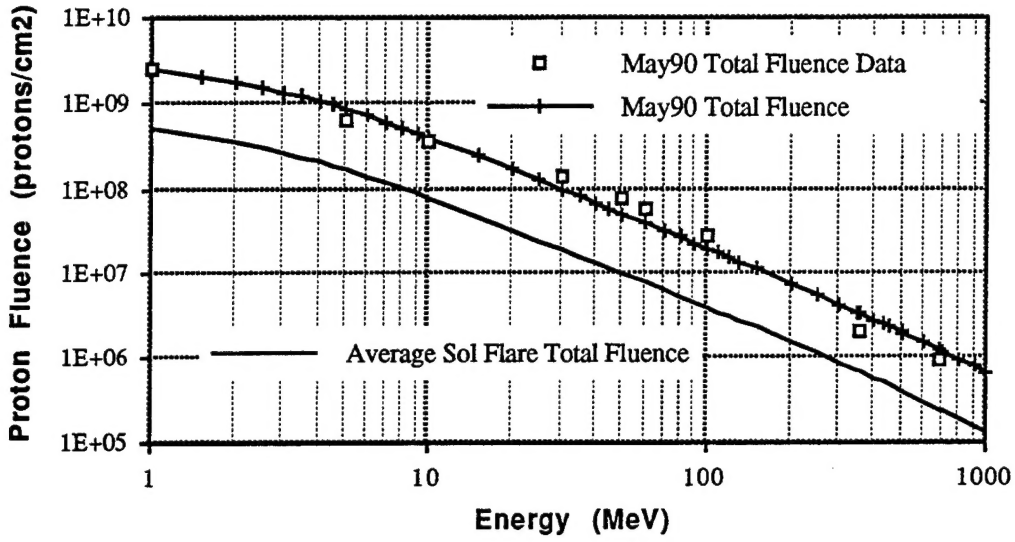

Figure B-2. Event Total Integral Fluence of May90 and Average Events

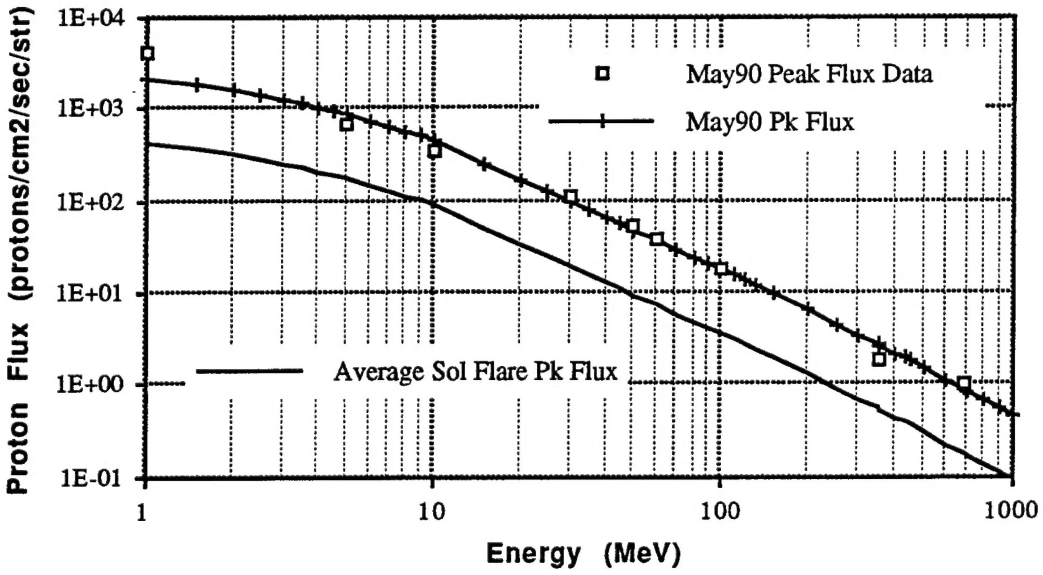

Figure B-3. Peak Integral Flux of May90 and Average Events

The event-total fluence and the peak flux of the average event are expressed as follows, where the proton rigidity, $R_p = \sqrt{E^2 + 2m_p E}$, is in units of megavolts, and the energy and proton mass, E and m_p, respectively, are in MeV.

(a) Event Total Integral Fluence of Average Event in units of (protons/cm^2):

$$F = 1.15\times10^{9}\times exp(-R_p/51), \quad 1 \le E \le 10\,MeV$$
$$= 2.30\times10^{13}\times R_p^{-2.55}, \quad 10 < E \le 1000\,MeV \qquad \text{(B-1)}$$

(b) Peak Integral Flux of Average Event in units of (protons/cm^2/sec/str):

$$J = 8.94\times10^{2}\times exp(-R_p/60), \quad 1 \le E \le 10\,MeV$$
$$= 6.47\times10^{7}\times R_p^{-2.74}, \quad 10 < E \le 1000\,MeV \qquad \text{(B-2)}$$

References

1. J. B. Blake and R. Mandel, "On-Orbit Observations of Single Event Upset in Harris HM-6508 1K RAMs," *IEEE Trans. Nucl. Sci.* **NS-33**, 1616–1619 (1986).

2. R. J. Ferro et al., "Multiple-bit Single Event Upset Study Team Report," Aerospace TOR-93(3461)-1, The Aerospace Corporation, El Segundo, CA (May 1993).

3. J. Feynman, G. Spitale, and J. Wang, "Interplanetary Proton Fluence Model: JPL 1991," *J. Geophys. Res.* **98**, 13,281–13,294 (1993).

4. H. H. Sauer, "GOES Observations of Energetic Protons to E>685 MeV: Ground-Level Events from October 1983 to July 1992," *Proceedings of the 23rd International Cosmic Ray Conference*, Vol. 3 (1992), p. 254; also H. H. Sauer, "GOES Observations of Energetic Protons to E>685 MeV: Description and Data Comparison," *Proceedings of the 23rd International Cosmic Ray Conference*, Vol. 3 (1992), p. 250.

5. J. B. Reagan et al., *Characteristics of the August 1972 Solar Particle Events as Observed over the Earth's Polar Caps*, LMSC/D352207 (June 1973).

6. *SPACE RADIATION*, V.2.5, commercial code marketed by Severn Communications Corporation.

7. J. H. Adams et al., *Cosmic Ray Effects on Microelectronics, Part I: The Near-Earth Particle Environment*, NRL Memorandum 4506 (25 August 1981); also, J. H. Adams, *Cosmic Ray Effects on Microelectronics*, Part IV, NRL Memorandum Report 5901 (31 December 1986) (Revised 31 December 1987).

8. D. L. Chenette and W. F. Dietrich, "The Solar Flare Heavy Ion Environment for Single-Event Upsets: a Summary of Observations over the Last Solar Cycle, 1973-1983," *IEEE Trans. Nucl. Sci.* **NS-31**, 1217–1222 (1984).

9. J. H. King., "Solar Proton Fluences for 1977–1983 Space Missions," *J. Spacecraft* **11**, 401–408 (1974).

10. T. J. Lie, "Multiple-bit Single Event Upsets of Microelectronic Memory," Aerospace TOR-92(2530)-1, The Aerospace Corporation, El Segundo, CA (April 1992).

11. *NOAA Compact Disk GOES-7 Data.*

TECHNOLOGY OPERATIONS

The Aerospace Corporation functions as an "architect-engineer" for national security programs, specializing in advanced military space systems. The Corporation's Technology Operations supports the effective and timely development and operation of national security systems through scientific research and the application of advanced technology. Vital to the success of the Corporation is the technical staff's wide-ranging expertise and its ability to stay abreast of new technological developments and program support issues associated with rapidly evolving space systems. Contributing capabilities are provided by these individual Technology Centers:

Electronics Technology Center: Microelectronics, VLSI reliability, failure analysis, solid-state device physics, compound semiconductors, radiation effects, infrared and CCD detector devices, Micro-Electro-Mechanical Systems (MEMS), and data storage and display technologies; lasers and electro-optics, solid state laser design, micro-optics, optical communications, and fiber optic sensors; atomic frequency standards, applied laser spectroscopy, laser chemistry, atmospheric propagation and beam control, LIDAR/LADAR remote sensing; solar cell and array testing and evaluation, battery electrochemistry, battery testing and evaluation.

Mechanics and Materials Technology Center: Evaluation and characterization of new materials: metals, alloys, ceramics, polymers and composites; development and analysis of advanced materials processing and deposition techniques; nondestructive evaluation, component failure analysis and reliability; fracture mechanics and stress corrosion; analysis and evaluation of materials at cryogenic and elevated temperatures; launch vehicle fluid mechanics, heat transfer and flight dynamics; aerothermodynamics; chemical and electric propulsion; environmental chemistry; combustion processes; spacecraft structural mechanics, space environment effects on materials, hardening and vulnerability assessment; contamination, thermal and structural control; lubrication and surface phenomena; microengineering technology and microinstrument development.

Space and Environment Technology Center: Magnetospheric, auroral and cosmic ray physics, wave-particle interactions, magnetospheric plasma waves; atmospheric and ionospheric physics, density and composition of the upper atmosphere, remote sensing using atmospheric radiation; solar physics, infrared astronomy, infrared signature analysis; effects of solar activity, magnetic storms and nuclear explosions on the earth's atmosphere, ionosphere and magnetosphere; effects of electromagnetic and particulate radiations on space systems; space instrumentation; propellant chemistry, chemical dynamics, environmental chemistry, trace detection; atmospheric chemical reactions, atmospheric optics, light scattering, state-specific chemical reactions and radiative signatures of missile plumes, and sensor out-of-field-of-view rejection.